

Physicochemical Characterization of *n*-Butyl-3-methylpyridinium Dicyanamide Ionic LiquidIsabel Bandrés,[†] Beatriz Giner,[†] Ignacio Gascón,[†] Miguel Castro,[‡] and Carlos Lafuente^{*,†}

Departamento de Química Orgánica—Química Física, Facultad de Ciencias, Universidad de Zaragoza, 50009 Zaragoza, Spain, and Instituto de Ciencia de Materiales de Aragón, Universidad de Zaragoza-CSIC, 50018 Zaragoza, Spain

Received: July 2, 2008; Revised Manuscript Received: August 1, 2008

The room temperature ionic liquid *n*-butyl-3-methylpyridinium dicyanamide has been characterized. Physicochemical properties such as density, speed of sound, refractive index, surface tension, and kinematic viscosity of the studied liquid have been experimentally measured in a wide range of temperatures. From results, coefficients of thermal expansion, molar refractions, dynamic viscosities and entropies and enthalpies of surface formation per unit surface area at the studied temperatures have been derived. We have analyzed the achieved results for evaluating the effect of the anionic structure in these properties, getting interesting results which lead us to a better understanding of the behavior of the ions in the fluids. Moreover, thermal properties of several pyridinium-based ionic liquids have been investigated. Finally, from both dynamic viscosity values and glass transition temperature of the studied liquids, a detailed analysis of the behavior in fragility terms has been performed.

Introduction

The development of environmentally benign chemical products and transformations is the challenge of the “green chemistry”. Within this wide area that claims for a sustainable chemistry, researchers try to find the best medium for carrying out synthetic transformation, avoiding whenever possible the use of auxiliary substances like organic solvents due to the adverse effects they produce in the surroundings. Because the high volatility of organic compounds facilitates some of their solvent applications, such as their removal of reaction products, a large amount of the solvent is released into the atmosphere, forming low-level ozone and smog through free radical air oxidation processes, or into effluent water. An alternative to classical solvents that is acquiring currently a great importance is the use of room temperature ionic liquids (RTILs). The major advantage of using these types of compounds is their low vapor pressure, which is related to the Coulombic interactions between their constituents. Furthermore, RTILs can often act as both catalyst and solvent, which have caused them to be very important from an application point of view.^{1,2} Moreover, as they are generally characterized as being nonflammable and nontoxic and present high thermal, chemical, and electrochemical stability,³ RTILs have attracted worldwide scientific interest.

Despite ionic liquids having been known for many years, their investigation is relatively recent and therefore information on their properties is somewhat limited or incomplete. These compounds are liquids at low temperature, because the ions that constitute these RTILs are relatively large, asymmetric, and diffusely charged, leading to a poor molecular packing. Taking this into account, the combinations of different cationic and anionic structures, with at least one of those having organic nature, make the number of ionic liquids that could be formed swiftly increase. The most commonly studied ionic liquids are

based on imidazolium cations^{3–7} combined with different anions, such as hexafluorophosphate, tetrafluoroborate, or halide. The pyridinium-based ionic liquids constitute a very interesting family of compounds, since they exhibit a specially high thermal stability and constitute a lower cost alternative to imidazolium-based ionic liquids.⁸ A detailed review of the literature has shown that the number of works about this attractive type of RTILs is minor compared with that of imidazolium liquids, and for this reason we are involved in the study of them.

With the aim of increasing the understandings of the unusual characteristics of the RTILs, numerous studies on their physical properties, such as density, thermal behavior, or ionic conductivity, have been carried out.^{9–13} The knowledge of the properties of these compounds is of great importance, since it is the required beginning of a comprehensive study of their features depending on the ionic structures and the intermolecular interactions that are responsible for the behavior of these fluids. Furthermore, the accumulation of physical data for these substances is an essential step to choose or evaluate an RTIL for a particular application, that is, their actual potential as solvents can be realized.

In this work, we present the thermophysical properties of a RTIL, *n*-butyl-3-methylpyridinium dicyanamide ([b3mpy][N(CN)₂]), which is depicted in Figure 1. Density, speed of sound, refractive index, surface tension, and kinematic viscosity of the studied RTIL have been experimentally measured. Since one of the most attractive features of these compounds is the extended temperature range of the liquid-state behavior they offer, it is important to understand the effect of the temperature on the liquid properties.¹⁴ For this reason, measurements were carried out in a broad range of temperatures from 278.15 to 328.15 K. From the experimental results, we have obtained coefficients of thermal expansion, molar refractions, and dynamic viscosities at the studied temperatures. Moreover, we have calculated entropies and enthalpies of surface formation per unit surface area. Results have been compared to those obtained for *n*-butyl-3-methylpyridinium tetrafluoroborate ([b3mpy][BF₄]), an ionic liquid with the same cation and dissimilar anion that we have investigated previously.¹⁵ The differences have

* Author to whom correspondence should be addressed. Phone: +34-976-762295. Fax: +34-976-761202. E-mail: celadi@unizar.es.

[†] Universidad de Zaragoza.

[‡] Universidad de Zaragoza-CSIC.

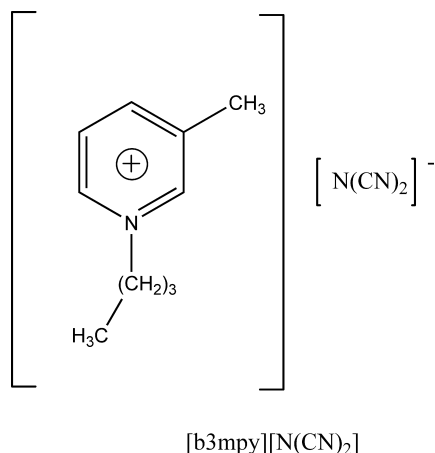


Figure 1. Structure and abbreviation of the ionic liquid under study.

been analyzed by paying attention to the change in the anionic structure and the consequences thereof. We have found only one reference of density of the liquid under study at room temperature.¹⁶

Furthermore, in order to complete the systematic characterization of several pyridinium-based ionic liquids which we have initialized,^{15,17} thermal properties of [b3mpy][BF₄], [b3mpy][N(CN)₂], and *n*-octyl-3-methylpyridinium tetrafluoroborate ([o3mpy][BF₄]) have been obtained in the 120–350 K temperature range. A detailed revision of literature has shown that only the glass transition temperature for [b3mpy][BF₄] has been reported before.¹² We have combined dynamic viscosity values and glass transition temperatures of the studied RTILs to perform an exhaustive analysis of their fragility based on the effect of the variations in their ionic structures.

Experimental Section

The room temperature ionic liquids *n*-butyl-3-methylpyridinium tetrafluoroborate (99%), *n*-butyl-4-methylpyridinium tetrafluoroborate (99%), *n*-octyl-3-methylpyridinium tetrafluoroborate (98%), and *n*-butyl-3-methylpyridinium dicyanamide (98%) were provided by Solvent Innovation. With the aim of decreasing the water content as much as possible, the RTILs were dried for 24 h under a vacuum of ca. 0.05 kPa with stirring and stored before use in a desiccator. Measurements were performed in a range of temperatures from 278.15 to 328.15 K with an interval of 2.5 K between each temperature, except in the case of refractive index, whose measurements were carried out from 283.15 to 328.15 K.

Densities, ρ , of the pure compounds were determined with an Anton Paar DMA-58 vibrating tube densimeter automatically thermostated within ± 0.01 K. The calibration was carried out with deionized doubly distilled water and dry air. In order to reduce the uncertainties in the density values due to the significant viscosity which this liquid presents, we have used the correction factor recommended by Anton Paar.^{18,19} The final uncertainty of density is estimated to be $\pm 10^{-4}$ g cm⁻³.

Speeds of sound, u , were obtained with an Anton Paar DSA-48 vibrating tube densimeter and sound analyzer. The temperature was automatically kept constant within ± 0.01 K. The uncertainty of the speed of sound is ± 0.1 m s⁻¹. Calibration of the apparatus was carried out with air and deionized double-distilled water.

Refractive indices, n_D , at 589.3 nm sodium D wavelength were measured using a high precision automatic refractometer (Abbemat-HP DR, Kernchen) whose temperature was internally

controlled within ± 0.01 K. The apparatus was calibrated with deionized double-distilled water. The corresponding uncertainty is $\pm 1 \times 10^{-6}$.

Surface tensions, σ , were determined using a drop volume tensiometer (Lauda TVT-2).²⁰ The temperature was kept constant within ± 0.01 K by means of an external Lauda E-200 thermostat. Details of the experimental procedure can be found elsewhere.²¹ The uncertainty of the surface tension measurement is ± 0.01 mN m⁻¹ of the final value of surface tension.

Kinematic viscosities, ν , were determined using an Ubbelohde viscosimeter with a Schoot-Geräte automatic measuring unit (model AVS-440). CaCl₂ drying tubes were used to protect the samples from moisture in the air. The temperature was kept constant within ± 0.01 K by means of a Schoot-Geräte thermostat. The viscosimeter constant was provided by the supplier and was $K = 0.9822$ mm² s⁻². The uncertainty of the time flow measurements is ± 0.01 s, and the corresponding uncertainty in the kinematic viscosity is ± 0.01 mm² s⁻¹. From density and kinematic viscosity, the absolute viscosity, η , can be obtained as $\eta = \rho\nu$, and the estimated uncertainty in the absolute viscosity is ± 0.01 mPa s.

DSC experiments were performed in the 120–350 K temperature range, using a differential scanning calorimeter Q1000 from TA Instruments with the LNCS accessory in order to reach the low-temperature range. The experiments were performed in a helium gas atmosphere. The measurements were carried out using $2\text{--}5 \pm 0.01$ mg of sample sealed at room temperature in aluminum pans with a mechanical crimp. Temperature and enthalpy calibrations were made with standard samples of indium, using its melting transition (429.76 K, 3.296 kJ mol⁻¹), and with a sample of Mn₃GaC, using its ferro- to antiferromagnetic transition (171.83 K, 713 J mol⁻¹). These calibration measurements allow us to estimate an overall uncertainty of ± 0.5 K in temperature and $\pm 2\%$ in enthalpy contents. The measurements for each RTIL were done using the following procedure: The sample after the drying vacuum process was exposed to the air only a few minutes in order to seal them in the aluminum pan. Once inside the DSC furnace, the sample was cooled from room temperature down to 120 K at 10 K/min, and after the thermal equilibrium was reached, a heating process was performed up to 350 K at 10 K/min.

The reported glass transition temperature, T_g , has been obtained from the midpoint of the small heat capacity jump on heating, corresponding to the transformation from amorphous glass state to a liquid state. On the other hand, the melting temperature has been taken to be the onset of an endothermic peak on heating, whereas the cold crystallization temperature has been determined as the onset of an exothermic peak on heating from a subcooled liquid state to a crystalline solid state. Both phenomena overlap in temperature in the [b3mpy][N(CN)₂] compound; therefore, it is difficult to estimate the melting and cold crystallization temperature and enthalpy contents of both processes.

Results and Discussion

Physicochemical Properties. The different molecular effects that characterize a compound are reflected with more or less intensity depending on the studied property. For example, taking into account the results obtained from molar refraction and speeds of sound, we can achieve a general idea of the structural organization of ions. From previous studies^{22,23} we could suggest that surface tension relies strongly on bulk interactions, even though the molecular orientation in the surface is also very important. Nevertheless, viscosity not only depends on interac-

TABLE 1: Fitting Parameters and Standard Deviations for the Studied Properties for [b3mpy][N(CN)₂]

property	A	B	s
$\rho/\text{g cm}^{-3}$	-0.000599	1.2276	0.0002
n_D	-0.0003218	1.62968	0.00001
$u/\text{m s}^{-1}$	-2.43	2481	1
$\sigma/\text{mN m}^{-1}$	-0.0613	68.66	0.02

property	η_0	B	T_0	s
$\eta/\text{mPa s}$	0.2258	602.3	180.52	0.03

tions but also it is influenced by organization of ions and the ability of them to flow. For this reason, the results of a broad number of properties give us the possibility of obtaining a more complete vision of the behavior of these RTILs.

In order to investigate the correlation between the studied thermophysical properties and the different structures of the RTILs, we have compared the experimental values founded for [b3mpy][N(CN)₂] with those obtained previously for [b3mpy][BF₄].¹⁵ For each property, we have analyzed the differences between both liquids, trying to achieve the understanding of the variations in the features of the liquids with the anionic structure.

The results have been interpreted by taking into account several molecular factors, such as the size, shape, and structure of the ions, as well as energetic factors like Coulombic and van der Waals interactions. For this reason, it is important to consider several characteristics of the ions previous to this analysis. Although the anion tetrafluoroborate has a higher formula weight than the anion dicyanamide, the tabulated volume by Jenkins et al.²⁴ for the anion [BF₄]⁻ (73 Å³) seems to be somewhat lower than that derived by Ye et al.¹⁶ for the anion [N(CN)₂]⁻ (86 Å³) (note that authors estimate that the typical average error in the volume of a ion is 10–20 Å³). The fact that a higher formula weight does not correspond with a higher size could be related with the shape of anions. Thus, the more symmetric structure of the anion [BF₄]⁻ might cause the smaller size.

As expected,^{3,6,22} we have found a linear dependence of the thermodynamic properties with temperature in the range of the measurements for the liquid under study. Therefore, experimental data have been correlated with the following equation:

$$Y = AT + B \quad (1)$$

where Y is the studied property and A and B are adjustable parameters. The best linear fitting parameters and the standard deviations of each property are gathered in Table 1.

As shown in Figure 2, the density of [b3mpy][N(CN)₂] decreases linearly with temperature. Moreover, we note that values are clearly smaller than those obtained for [b3mpy][BF₄] and the majority of RTILs studied earlier,^{3–7} being comparable to density of common organic solvents. In this case, density increases when the formula weight of the anion does. In previous works, the same conclusions have been obtained when the dependence on density with anions has been analyzed.^{3,6} As we have mentioned before, we have found a density value for [b3mpy][N(CN)₂] at room temperature that agrees with our experimental values.¹⁶

A useful thermodynamic property, the coefficient of thermal expansion, α , can be determinate from experimental data of density. Values of the coefficient decrease faintly when the temperature increases, and at $T = 298.15$ K, it shows a value of $\alpha = 5.74 \times 10^{-4} \text{ K}^{-1}$. Although both [b3mpy][N(CN)₂] and [b3mpy][BF₄] exhibit quite different values of densities, the

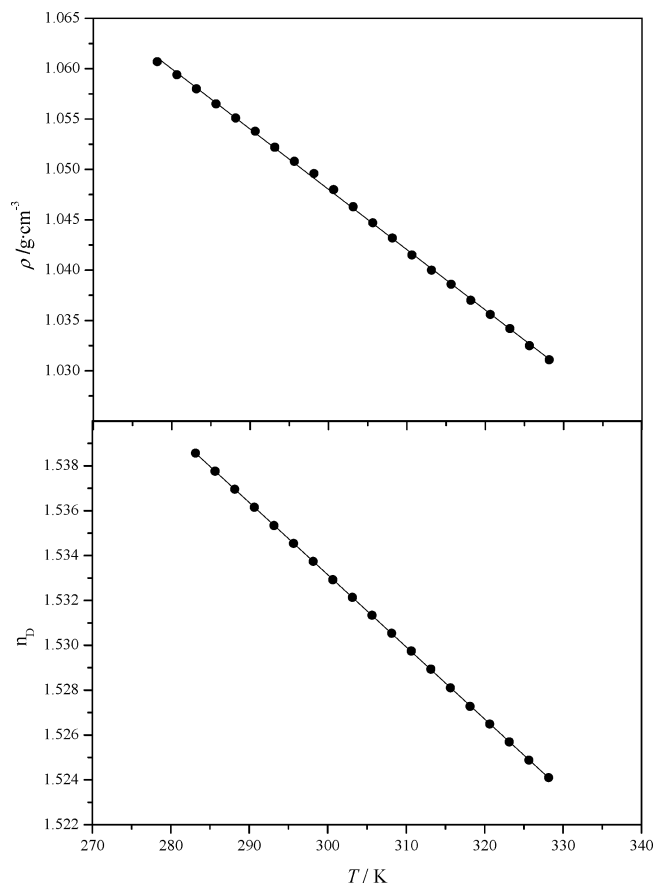


Figure 2. Density and refractive index as a function of temperature for [b3mpy][N(CN)₂]. Continuous lines are calculated values using eq 1.

behavior of them with temperature is very similar. For this reason, the differences in the coefficients of thermal expansion are slight. These values are comparable to coefficients obtained in other ionic liquids like [b4mpy][BF₄] ($5.72 \times 10^{-4} \text{ K}^{-1}$)¹⁵ or 1-ethyl-3-methylimidazolium aminoacetate ($5.20 \times 10^{-4} \text{ K}^{-1}$).¹³

Refractive indices are represented in Figure 2. In the light of the results, we can say that this property decreases linearly with temperature for [b3mpy][N(CN)₂]. Even though the values are visibly greater than those obtained for the [b3mpy][BF₄], both liquids undergo a similar change with temperature.

The molar refraction, R_m , of the liquid has been calculated from experimental data of both density and refractive index at all the studied temperatures using the Lorentz–Lorenz relation. The values are gathered in the Supporting Information. As is known, molar refraction is considered the hard core volume of 1 mol of molecules. We have found that not only is the free molar volume higher for [b3mpy][BF₄] than for [b3mpy][N(CN)₂], but the hard core volume for [b3mpy][N(CN)₂] is also much greater than that calculated for [b3mpy][BF₄], since the former exhibits larger molar refraction values. This implies that ions that form part of [b3mpy][N(CN)₂] have a more packed structure than ions in [b3mpy][BF₄], that is, the anion [N(CN)₂]⁻ could facilitate a better organization in the fluid than [BF₄]⁻. This might be related to the fact that the anion dicyanamide is more coordinating than other common anions present in this type of fluid, such as [BF₄]⁻.²⁵ Taking into account the volumetric behavior described earlier, which seems to indicate a more packed structure for the ionic liquid [b3mpy][N(CN)₂], it is not enough to counterbalance the effect of the decrease of the formula weight of the anion.

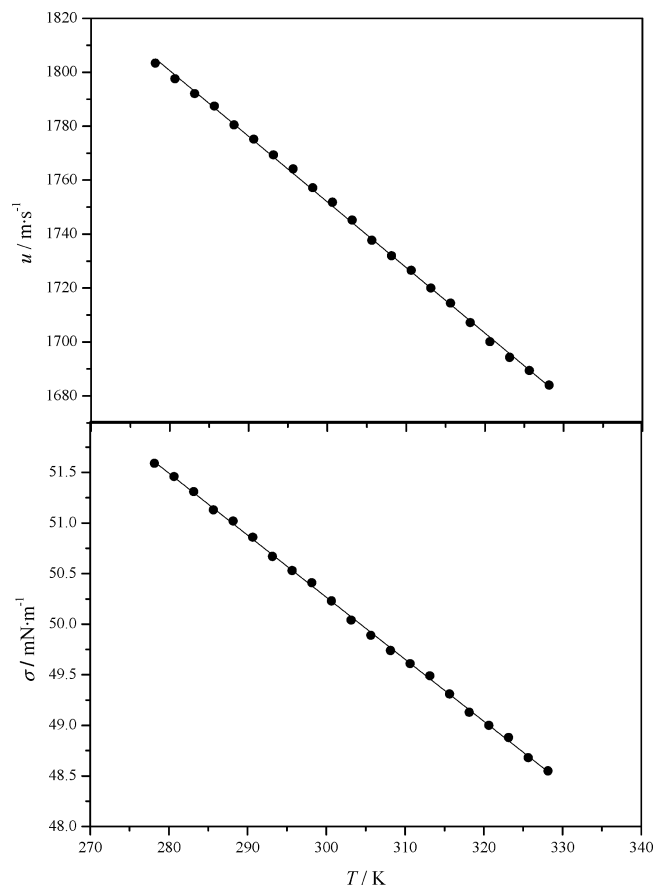


Figure 3. Speed of sound and surface tension as a function of temperature for [b3mpy][N(CN)₂]. Continuous lines are calculated values using eq 1.

As can be seen in Figure 3, speeds of sound values diminish when temperature increases. In the same way, refractive index values for [b3mpy][N(CN)₂] are greater than those for [b3mpy][BF₄]. This is in agreement with the conclusions reached earlier about the better organization of the ions for [b3mpy][N(CN)₂].

Surface tension values for the studied liquid decrease with temperature, as is shown in Figure 3. Even though information about this property for RTILs is not very extensive, there are several works^{22,23} that give some explanations about the behavior of the surface tension in order to find its dependence on different molecular parameters. One of them²² is based on the structure and surface orientation of ions. It is related to the fact that despite the interface being constituted of both cations and anions in order to preserve the electroneutrality, the overall surface tension could reflect primarily the properties of the cations modified by those of the anions, due to the larger size of the former ions. However, in the light of the experimental values for [b3mpy][N(CN)₂] and [b3mpy][BF₄], which share the same cation, we pointed out that the influence of the anion on this property seems to be very significant. Some other studies²³ propose that, apart from the orientation of the ions in the surface, intermolecular interactions that can occur not only in the interface but also in the bulk have a great influence on this property. Within molecular interactions that can appear in pyridinium-based ionic liquids, the van der Waals and Coulomb interactions are the most important. Their contributions change, depending on different molecular effects, such as the shape, size, or charge of the ions that form part of the fluid, the actual surface tension value being a sign of the type of the predominant

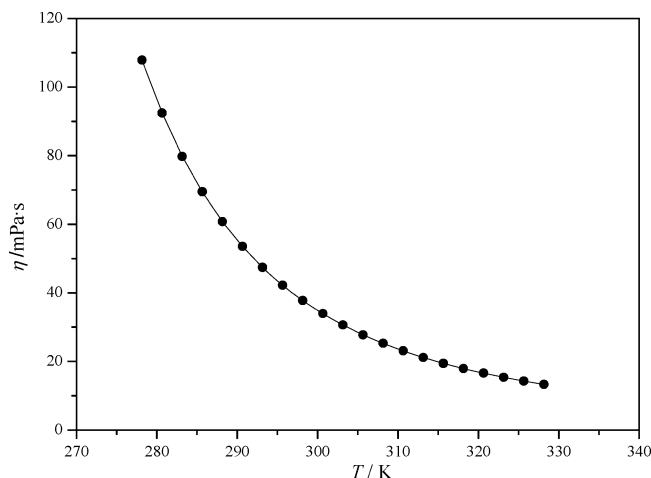


Figure 4. Dynamic viscosity as a function of temperature for [b3mpy][N(CN)₂]. (—) Plot of the Vogel–Fulcher–Tamman equation.

interaction. Therefore, from the experimental results of the present work, we can say that interactions have more importance in [b3mpy][N(CN)₂] than in [b3mpy][BF₄], showing that when the formula weight of the anion decreases, the surface tension increases.

From the experimental surface tension data, the entropy and enthalpy of surface formation per unit surface area can be calculated. The entropy of surface formation per unit surface area is independent of temperature, since experimental values are related linearly in the range of the measurements and has a value of $\Delta S = 0.06 \text{ mN m}^{-1} \text{ K}^{-1}$ for the ionic liquid [b3mpy][N(CN)₂]. The enthalpy of surface formation per unit area changes slightly with temperature and has a value of $\Delta H = 68.69 \text{ mN m}^{-1}$ at 298.15 K. Comparing the surface quantities, we show that entropy of surface formation is smaller for [b3mpy][N(CN)₂] than for [b3mpy][BF₄], whereas we found the opposite results for the enthalpy of surface formation. Law et al.²² and Freire et al.²³ pointed out that lower values of entropy of surface formation could indicate an enhancement of the degree of surface orientation. Therefore, the anion [N(CN)₂][−] could cause a better orientation of the ions into the surface than in the case of [BF₄][−] anions.

As shown in Figure 4, the temperature dependence on the dynamic viscosity values presents convex-curved profiles, and consequently, data were fitted to the Vogel–Fulcher–Tamman equation:^{26–28}

$$\eta = \eta_0 \exp[B/(T - T_0)] \quad (2)$$

where η_0 , B , and T_0 are the adjustable parameters collected in Table 1.

Results show that dynamic viscosity decreases significantly with temperature at low temperatures until a gentle descent is achieved at high temperatures. Experimental data of this property are smaller than those obtained for [b3mpy][BF₄], getting the greatest differences between them at low temperatures.

Previous studies²⁹ have analyzed the dependency of ionic structures in viscosity data. When cationic structures were studied, the larger size and molecular weight cause the larger viscosity values. However, when the effect of the anion size was considered, a correlation was not found.

From an evaluation of the results of both compounds, we observe that dynamic viscosity is strongly affected by the nature of the ions that constituent the RTILs; in this case, an increase of the formula weight of the anion results in an increase of the

TABLE 2: Glass Transition (T_g), Cold Crystallization (T_{cc}), and Melting (T_m) Temperatures for the Studied RTILs

compd	T_g /K	T_{cc} /K	T_m /K
[b3mpy][BF ₄]	194		
[b4mpy][BF ₄]	203		
[o3mpy][BF ₄]	201		
[b3mpy][N(CN) ₂]	185	234	278

property. It could be explained by attending to molecular factors such as interactions between the involved ions, the size or the shape of them, and their organization in the bulk. As we have mentioned before, the van der Waals and Coulomb interactions are the most important, and the relevance of each type of interaction depends on the size of the ions and their relation to the surroundings, which is related to the possibility of forming ion pairs and neutral aggregates. The final viscosity value observed is a reflection of all the factors mentioned before that have to be taken into account to describe the behavior of this transport property.^{25,29}

Values of density, speed of sound, refractive index, molar refraction, surface tension, kinematic viscosity, and dynamic viscosity of the ionic liquid *n*-butyl-3-methylpyridinium dicyanamide at the studied temperatures can be found in the Supporting Information.

Thermal Properties. Thermal properties of the pyridinium-based ionic liquids [b3mpy][BF₄], [b4mpy][BF₄], [o3mpy][BF₄], and [b3mpy][N(CN)₂] have been investigated by differential scanning calorimetry. Experimental values of the different temperatures are collected in Table 2.

Among the studied RTILs, two types of thermal behaviors have been detected. The first group ([b3mpy][BF₄], [b4mpy][BF₄], and [o3mpy][BF₄]) is characterized by the formation of an amorphous glass at low temperatures. These compounds do not form a crystalline phase; thus, their DSC thermograms do not present melting points but only glass transition temperatures. The heating thermogram, shown in Figure 5 for the [b3mpy][BF₄] ionic liquid (scan 2), illustrates this behavior. The experimental value of the glass transition temperature for [b3mpy][BF₄] is in good agreement with that obtained earlier by Crosthwaite et al.¹² In the second type of behavior, the RTIL ([b3mpy][N(CN)₂]) remains liquid upon cooling until it reaches an amorphous glass state at low temperatures. Nevertheless, a cold crystallization occurs when the compound is heated above T_g ; i.e., the subcooled liquid forms a crystalline solid. Structural rearrangements driven by an increase of the molecular mobility can be the origin of this thermal behavior.¹⁰ Finally, the solid melts at T_m . The heating scan for the [b3mpy][N(CN)₂] compound (scan 1) is depicted in Figure 5. In this case, it is possible to calculate the transitions of melting and cold crystallization enthalpy, which are 12.11 and 11.46 kJ mol⁻¹ K⁻¹, respectively. As expected, calculated enthalpies for both phase transitions are similar. The ionic liquid [b3mpy][N(CN)₂] seems to confirm satisfactorily an empirical rule that connects the glass transition temperature to the melting point, the $T_g/T_m \approx 2/3$ rule.

Fragility Analysis. The term known as fragility makes reference to the rate at which the transport properties change with temperature near to the glass transition point. This property provides a useful way to classify the compounds depending on the different viscosity–temperature relations that they exhibit. Thus, in order to define the range in which all available experimental results fall, the adjectives strong and fragile have been suggested for representing the extremes of the behavior that these compounds may present.

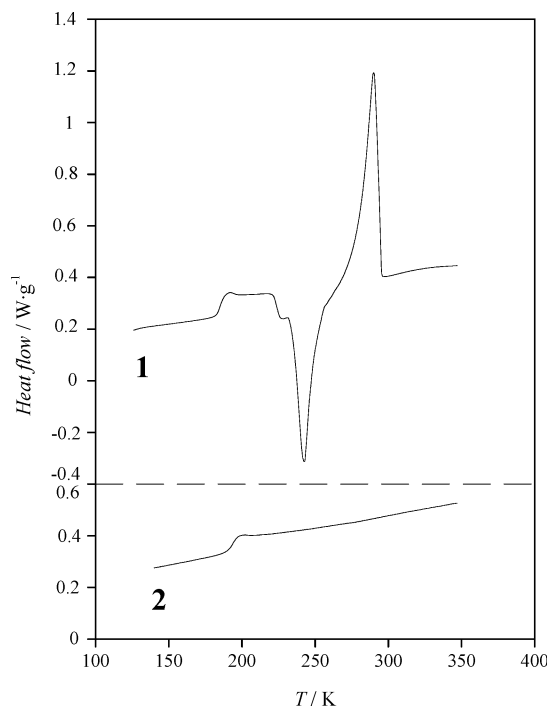


Figure 5. Differential scanning calorimetry results for [b3mpy][N(CN)₂] (1) and for [b3mpy][BF₄] (2).

The fragile compounds show an extreme temperature dependence near the glass transition point. They commonly present nondirectional bonds and often exhibit ionic or aromatic character. On the other hand, strong systems are observed to be those with self-reinforcing tetrahedral network structures, showing a strong resistance against structural degradation when heated through their supercooled regime.^{30,31}

The diagram that represents the logarithm of viscosity as a function of (T_g/T) has become the basis of the classification, allowing a visual evaluation of the liquids through an analysis of the deviations from Arrhenius behavior. Thus, the most fragile materials are those that show the largest deviation, falling on the right-hand side of the plot. In contrast, the representation of a strong compound is hard to distinguish from that of the Arrhenius law. Moreover, to classify the compounds between these extreme behaviors from available experimental results, others parameters can be taken into account. The Vogel–Fulcher–Tamman equation^{26–28} of viscosity is an empirical expression that describes viscosity over many orders of magnitude with a good accuracy.³² It contains specific constants, η_0 , B , and T_0 that, as we have mentioned before, are determined by fitting eq (2) to experimental data. From these parameters, the strength parameter $D = B/T_0$ can be calculated. D is related³³ to the fragility in the classification proposed by Angell, where a D value less than 10 represents a fragile behavior whereas values of the strength parameter are around 100 for strong liquids.³⁰ It has been found that the pattern graphically obtained can be reproduced by the variations of the single parameter D .

Since both dynamic viscosity values and the glass transition temperature of the studied RTILs have been experimentally measured, in this work a detailed analysis of the behavior in fragility terms can be performed. Thus, the effect of the position of the substituents, the alkyl chain length in pyridinium cations, and the anions have been analyzed by means of the comparison of the properties of [b3mpy][BF₄] with those exhibited by [b4mpy][BF₄], [o3mpy][BF₄], and [b3mpy][N(CN)₂], respectively.

Results have been represented in different ways to compare the behavior of these liquids. In Figure 6, experimental values

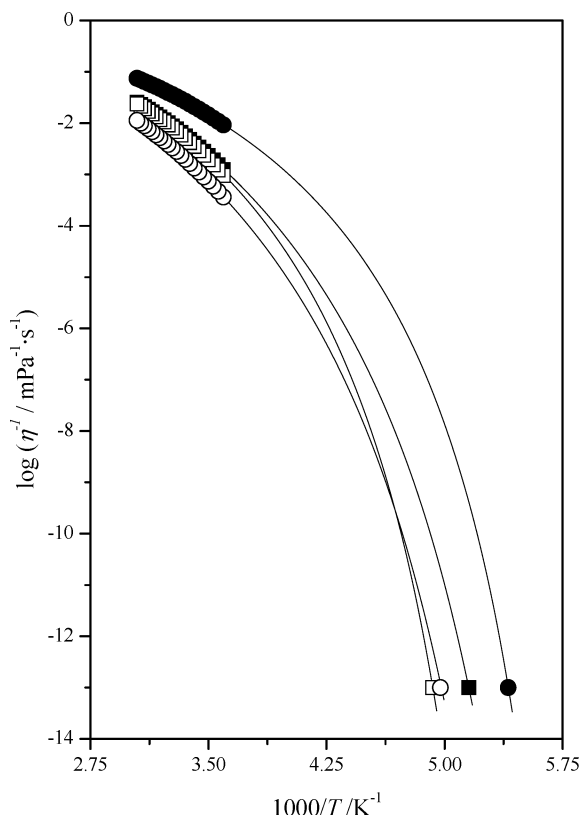


Figure 6. Arrhenius plot of fluidities of [b3mpy][BF₄] (■), [b4mpy][BF₄] (□), [o3mpy][BF₄] (●), and [b3mpy][N(CN)₂] (○) on an expanded scale to include values at the glass-transition temperature. (—) Plot of the Vogel–Fulcher–Tamman equation.

for fluidities, φ , defined as the inverse of the dynamic viscosity of the studied RTILs in the common Arrhenius form, are shown. In order to plot the fluidity over the whole liquid range for these liquids, Figure 6 includes for each RTIL the value at its onset point, defined as the glass transition temperature. The fluidity in this point is the inverse of the viscosity that has been found for common liquids whose T_g values are below of room temperature ($\eta \approx 10^{13}$ mPa s).³⁴ Note that experimental data have been fitted to the Vogel–Fulcher–Tamman equation for viscosity.^{26–28} Moreover, the behavior of the RTILs can be compared by means of the T_g -scaled Arrhenius plots of viscosities, which are represented in Figure 7.

From the analysis of Figure 7, it is worth noting that the studied RTILs show a similar temperature dependence on viscosity, showing small differences between their plots. Furthermore, viscosity data are situated on the right-hand side of the diagram, indicating greater deviations from Arrhenius behavior. These results suggest that the studied RTILs are fragile, being in a close position to some molten nitrates or newly organic compounds that are representative of the fragility edge. Taking into account their situation in Figure 7, the sequence [b3mpy][N(CN)₂] > [b4mpy][BF₄] > [b3mpy][BF₄] > [o3mpy][BF₄] is presented in terms of their fragility. Although actually it is not clear which are the factors that control the fragility, we can suggest a series of interpretations attending to their structural characteristics. In this way, the analysis of the properties for [b3mpy][BF₄] and [b4mpy][BF₄] provides a general idea about how the features of the liquids are affected when the methyl group changes from position 3 in the ring to the position 4. In this case, the more symmetric structure of the cation gives rise to more fragile liquids. On the other hand, it has been found that [b3mpy][N(CN)₂] is the most fragile of

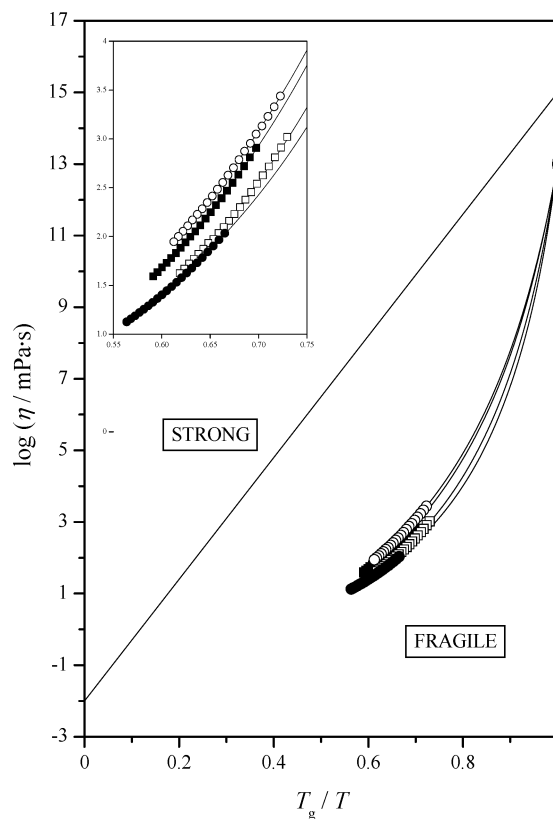


Figure 7. T_g -scaled Arrhenius plots of viscosities of [b3mpy][BF₄] (■), [b4mpy][BF₄] (□), [o3mpy][BF₄] (●), and [b3mpy][N(CN)₂] (○). The inset shows an enlargement of the experimental data. (—) Plot of the Vogel–Fulcher–Tamman equation.

TABLE 3: Adjustable Parameters, B and T_0 , of the Vogel–Fulcher–Tamman Equation and the Calculated D for the Studied Compounds

compd	B/K	T_0/K	D
[b3mpy][BF ₄]	936.810 ^a	176.5069 ^a	5.31
[b4mpy][BF ₄]	758.922 ^a	191.6670 ^a	3.96
[o3mpy][BF ₄]	1255.83 ^b	165.541 ^b	7.59
[b3mpy][N(CN) ₂]	602.304	180.5168	3.34

^a From ref 15. ^b From ref 17.

the analyzed RTILs. This indicates that the combination of the [b3mpy]⁺ cation with the [N(CN)₂][−] anion modifies the behavior of the liquids in the direction of increasing fragility. From the comparison between the behavior of [b3mpy][BF₄] and [o3mpy][BF₄], it is possible to suggest that an increase of the alkyl chain length in the pyridinium cation leads to less fragile systems. As expected, the order found for the D parameters calculated from specific constants of the Vogel–Fulcher–Tamman equation for each of the liquids is in good agreement with results derived from the T_g -scaled Arrhenius plot, being a probe that confirms that the sequence of the RTILs in based on their fragility. Values of the adjustable parameters and the calculated D for the studied compounds are collected in Table 3.

Conclusions

In this paper, the thermophysical properties of *n*-butyl-3-methylpyridinium dicyanamide have been investigated. Density, speed of sound, refractive index, surface tension, and kinematic viscosity of the studied liquid have been experimentally measured in a broad range of temperatures, and from the experimental results, coefficients of thermal expansion, molar

refractions, dynamic viscosities, and entropies and enthalpies of surface formation per unit surface area at the studied temperatures have been obtained. The present study contributes to a better understanding of the structure–property relationship of this type of fluid, which is fundamental to evaluate the suitability of these compounds for industrial applications. Results have been compared with those obtained previously for *n*-butyl-3-methylpyridinium tetrafluoroborate to analyze the effect of the anionic structure on the behavior of the pyridinium-based ionic liquids. In the light of the results, we have found that density and dynamic viscosity are strongly affected by nature of the ions, resulting in an increase of the property when the formula weight of the anion increases. Moreover, from both volumetric properties and refractive index results, we can affirm that the dicyanamide anion facilitates a better organization in the fluid than the tetrafluoroborate anion, information that is corroborated with results obtained from speed of sound. Surface tension values indicate that interactions have a greater importance in [b3mpy][N(CN)₂] than [b3mpy][BF₄] and suggest an increase of the degree of surface orientation.

On the other hand, calorimetric properties of the ionic liquids [b3mpy][BF₄], [b4mpy][BF₄], [o3mpy][BF₄], and [b3mpy][N(CN)₂] have been investigated, in order to complete their comprehensive characterization. The apparent fragility of these RTILs, derived from both experimental viscosity and glass transition temperatures, has been discussed in structural terms.

Acknowledgment. We are grateful for financial assistance from Ministerio de Educación y Cultura, Ministerio de Medio Ambiente (2007 0483), and from the Spanish Ministerio de Educación y Ciencia (MAT2007-61621). Authors are also indebted to Dirección General de Aragón and Universidad de Zaragoza for financial support (INFR 423-06). M.I.B. is thankful for the predoctoral fellowship from D.G.A.

Note Added after Print Publication. This paper was published on the Web on September 9, 2008, and in the October 2, 2008, issue. The word “Dicyanamide” was misspelled in the title and title running head. The electronic version was corrected and reposted to the Web issue on December 18, 2008. An Addition and Correction appears in the December 25, 2008, issue (Vol. 112, No. 51).

Supporting Information Available: Values of density, speed of sound, refractive index, molar refraction, surface tension, kinematic viscosity, and dynamic viscosity of the ionic liquid *n*-butyl-3-methylpyridinium dicyanamide. This material is available free of charge via the Internet at <http://pubs.acs.org>.

References and Notes

(1) Anastas, P. T.; Warner, J. C. *Green Chemistry: Theory and Practice*; Oxford University Press: New York, 1998.

- (2) Lancaster, M. *Green Chemistry: An Introductory Text*; The Royal Society of Chemistry: London, 2002.
- (3) Tokuda, H.; Hayamizu, K.; Ishii, K.; Hasan Susan, M. A. B.; Watanabe, M. *J. Phys. Chem. B* **2004**, *108*, 16593.
- (4) Tokuda, H.; Hayamizu, K.; Ishii, K.; Hasan Susan, M. A. B.; Watanabe, M. *J. Phys. Chem. B* **2005**, *109*, 6103.
- (5) Huddleston, J. G.; Visser, A. E.; Reichert, W. M.; Willauer, H. D.; Broker, G. A.; Rogers, R. D. *Green Chem.* **2001**, *3*, 156.
- (6) Fredlake, C. P.; Crosthwaite, J. M.; Hert, D. G.; Aki, S. N. V. K.; Brennecke, J. F. *J. Chem. Eng. Data* **2004**, *49*, 954.
- (7) Davila, M. J.; Aparicio, S.; Alcalde, R.; Garcia, B.; Leal, J. M. *Green Chem.* **2007**, *9*, 221.
- (8) Cadena, C.; Zhao, Q.; Snurr, R. Q.; Maginn, E. J. *J. Phys. Chem. B* **2006**, *110*, 2821.
- (9) Yoshida, Y.; Baba, O.; Saito, G. *J. Phys. Chem. B* **2007**, *111*, 4742.
- (10) Zhang, Q.; Li, Z.; Zhang, J.; Zhang, S.; Zhu, L.; Yang, J.; Zhang, X.; Deng, Y. *J. Phys. Chem. B* **2007**, *111*, 2864.
- (11) Tokuda, H.; Ishii, K.; Hasan Susan, M. A. B.; Tsuzuki, S.; Hayamizu, K.; Watanabe, M. *J. Phys. Chem. B* **2006**, *110*, 2833.
- (12) Crosthwaite, J. M.; Muldoon, M. J.; Dixon, J. K.; Anderson, J. L.; Brennecke, J. F. *J. Chem. Thermodyn.* **2005**, *37*, 559.
- (13) Yang, J.-Z.; Zhang, Q.-G.; Wang, B.; Tong, J. *J. Phys. Chem. B* **2006**, *110*, 22521.
- (14) Xu, W.; Cooper, E. I.; Angell, C. A. *J. Phys. Chem. B* **2003**, *107*, 6107.
- (15) Bandres, I.; Giner, B.; Artigas, H.; Royo, F. M.; Lafuente, C. *J. Phys. Chem. B* **2008**, *112*, 3077.
- (16) Ye, C.; Shreeve, J. M. *J. Phys. Chem. A* **2007**, *111*, 1456.
- (17) Bandres, I.; Giner, B.; Artigas, H.; Lafuente, C.; Royo, F. M. *J. Chem. Eng. Data* In press (DOI: 10.1021/jc8002095).
- (18) Fandiño, O.; Pensado, A. S.; Lugo, L.; Lopez, E. R.; Fernandez, J. *Green Chem.* **2005**, *7*, 775.
- (19) Lundstrum, R.; Goodwin, A. R. H.; Hsu, K.; Frels, M. F.; Caudwell, D. R.; Trusler, J. P. M. *J. Chem. Eng. Data* **2005**, *50*, 1377.
- (20) Miller, R.; Hofmann, A.; Hartmann, R.; Schano, K.-H.; Halbig, A. *Adv. Mater.* **1992**, *5*, 370.
- (21) Giner, B.; Cea, P.; Lopez, M. C.; Royo, F. M.; Lafuente, C. *J. Colloid Interface Sci.* **2004**, *275*, 284.
- (22) Law, G.; Watson, P. R. *Langmuir* **2001**, *17*, 6138.
- (23) Freire, M. G.; Carvalho, P. J.; Fernandes, A. M.; Marrucho, I. M.; Queimada, A. J.; Coutinho, J. A. P. *J. Colloid Interface Sci.* **2007**, *314*, 621.
- (24) Jenkins, H. D. B.; Roobottom, H. K. *Inorg. Chem.* **1999**, *38*, 3609.
- (25) Xu, W.; Wang, L.-M.; Nieman, R. A.; Angell, C. A. *J. Phys. Chem. B* **2003**, *107*, 11749.
- (26) Vogel, H. *Phys. Z.* **1921**, *22*, 645.
- (27) Fulcher, G. S. *J. Am. Ceram. Soc.* **1923**, *8*, 339.
- (28) Tamman, G.; Hesse, W. Z. *Anorg. Allg. Chem.* **1926**, *156*, 245.
- (29) Noda, A.; Hayamizu, K.; Watanabe, M. *J. Phys. Chem. B* **2001**, *105*, 4603.
- (30) Angell, C. A. *J. Non-Cryst. Solids* **1991**, *13*, 131–133.
- (31) Bohmer, R.; Ngai, K. L.; Angell, C. A.; Plazek, D. J. *J. Chem. Phys.* **1993**, *99*, 4201.
- (32) Ojovan, M. I.; Travis, K. P.; Hand, R. J. *J. Phys.: Condens. Matter* **2007**, *19*, 415107.
- (33) Ozdemir Kart, S.; Tomak, M.; Uludogan, M.; Çagin, T. *Turk. J. Phys.* **2006**, *30*, 319.
- (34) Moynihan, C. T.; Macedo, P. B.; Montrose, C. J.; Gupta, P. K.; DeBolt, M. A.; Dill, J. F.; Dom, B. E.; Drake, P. W.; Eastale, A. J.; Elterman, P. B.; Moeller, R. P.; Sasabe, H. A.; Wilder, J. A. *Ann. N.Y. Acad. Sci.* **1976**, *279*, 15.

JP805816X